

Moments of the Hadronic Mass Spectrum in Inclusive Semileptonic B Decays at Belle

- K. Abe,¹⁰ K. Abe,⁴⁶ N. Abe,⁴⁹ I. Adachi,¹⁰ H. Aihara,⁴⁸ M. Akatsu,²⁴ Y. Asano,⁵³
 T. Aso,⁵² V. Aulchenko,² T. Aushev,¹⁴ T. Aziz,⁴⁴ S. Bahinipati,⁶ A. M. Bakich,⁴³
 Y. Ban,³⁶ M. Barbero,⁹ A. Bay,²⁰ I. Bedny,² U. Bitenc,¹⁵ I. Bizjak,¹⁵ S. Blyth,²⁹
 A. Bondar,² A. Bozek,³⁰ M. Bračko,^{22,15} J. Brodzicka,³⁰ T. E. Browder,⁹ M.-C. Chang,²⁹
 P. Chang,²⁹ Y. Chao,²⁹ A. Chen,²⁶ K.-F. Chen,²⁹ W. T. Chen,²⁶ B. G. Cheon,⁴
 R. Chistov,¹⁴ S.-K. Choi,⁸ Y. Choi,⁴² Y. K. Choi,⁴² A. Chuvikov,³⁷ S. Cole,⁴³
 M. Danilov,¹⁴ M. Dash,⁵⁵ L. Y. Dong,¹² R. Dowd,²³ J. Dragic,²³ A. Drutskoy,⁶
 S. Eidelman,² Y. Enari,²⁴ D. Epifanov,² C. W. Everton,²³ F. Fang,⁹ S. Fratina,¹⁵
 H. Fujii,¹⁰ N. Gabyshev,² A. Garmash,³⁷ T. Gershon,¹⁰ A. Go,²⁶ G. Gokhroo,⁴⁴
 B. Golob,^{21,15} M. Grosse Perdekamp,³⁸ H. Guler,⁹ J. Haba,¹⁰ F. Handa,⁴⁷ K. Hara,¹⁰
 T. Hara,³⁴ N. C. Hastings,¹⁰ K. Hasuko,³⁸ K. Hayasaka,²⁴ H. Hayashii,²⁵ M. Hazumi,¹⁰
 E. M. Heenan,²³ I. Higuchi,⁴⁷ T. Higuchi,¹⁰ L. Hinz,²⁰ T. Hojo,³⁴ T. Hokuue,²⁴
 Y. Hoshi,⁴⁶ K. Hoshina,⁵¹ S. Hou,²⁶ W.-S. Hou,²⁹ Y. B. Hsiung,²⁹ H.-C. Huang,²⁹
 T. Igaki,²⁴ Y. Igarashi,¹⁰ T. Iijima,²⁴ A. Imoto,²⁵ K. Inami,²⁴ A. Ishikawa,¹⁰ H. Ishino,⁴⁹
 K. Itoh,⁴⁸ R. Itoh,¹⁰ M. Iwamoto,³ M. Iwasaki,⁴⁸ Y. Iwasaki,¹⁰ R. Kagan,¹⁴ H. Kakuno,⁴⁸
 J. H. Kang,⁵⁶ J. S. Kang,¹⁷ P. Kapusta,³⁰ S. U. Kataoka,²⁵ N. Katayama,¹⁰ H. Kawai,³
 H. Kawai,⁴⁸ Y. Kawakami,²⁴ N. Kawamura,¹ T. Kawasaki,³² N. Kent,⁹ H. R. Khan,⁴⁹
 A. Kibayashi,⁴⁹ H. Kichimi,¹⁰ H. J. Kim,¹⁹ H. O. Kim,⁴² Hyunwoo Kim,¹⁷ J. H. Kim,⁴²
 S. K. Kim,⁴¹ T. H. Kim,⁵⁶ K. Kinoshita,⁶ P. Koppenburg,¹⁰ S. Korpar,^{22,15} P. Križan,^{21,15}
 P. Krokovny,² R. Kulasiri,⁶ C. C. Kuo,²⁶ H. Kurashiro,⁴⁹ E. Kurihara,³ A. Kusaka,⁴⁸
 A. Kuzmin,² Y.-J. Kwon,⁵⁶ J. S. Lange,⁷ G. Leder,¹³ S. E. Lee,⁴¹ S. H. Lee,⁴¹
 Y.-J. Lee,²⁹ T. Lesiak,³⁰ J. Li,⁴⁰ A. Limosani,²³ S.-W. Lin,²⁹ D. Liventsev,¹⁴
 J. MacNaughton,¹³ G. Majumder,⁴⁴ F. Mandl,¹³ D. Marlow,³⁷ T. Matsuishi,²⁴
 H. Matsumoto,³² S. Matsumoto,⁵ T. Matsumoto,⁵⁰ A. Matyja,³⁰ Y. Mikami,⁴⁷
 W. Mitaroff,¹³ K. Miyabayashi,²⁵ Y. Miyabayashi,²⁴ H. Miyake,³⁴ H. Miyata,³² R. Mizuk,¹⁴
 D. Mohapatra,⁵⁵ G. R. Moloney,²³ G. F. Moorhead,²³ T. Mori,⁴⁹ A. Murakami,³⁹
 T. Nagamine,⁴⁷ Y. Nagasaka,¹¹ T. Nakadaira,⁴⁸ I. Nakamura,¹⁰ E. Nakano,³³ M. Nakao,¹⁰
 H. Nakazawa,¹⁰ Z. Natkaniec,³⁰ K. Neichi,⁴⁶ S. Nishida,¹⁰ O. Nitoh,⁵¹ S. Noguchi,²⁵
 T. Nozaki,¹⁰ A. Ogawa,³⁸ S. Ogawa,⁴⁵ T. Ohshima,²⁴ T. Okabe,²⁴ S. Okuno,¹⁶
 S. L. Olsen,⁹ Y. Onuki,³² W. Ostrowicz,³⁰ H. Ozaki,¹⁰ P. Pakhlov,¹⁴ H. Palka,³⁰
 C. W. Park,⁴² H. Park,¹⁹ K. S. Park,⁴² N. Parslow,⁴³ L. S. Peak,⁴³ M. Pernicka,¹³
 J.-P. Perroud,²⁰ M. Peters,⁹ L. E. Piilonen,⁵⁵ A. Poluektov,² F. J. Ronga,¹⁰ N. Root,²
 M. Rozanska,³⁰ H. Sagawa,¹⁰ M. Saigo,⁴⁷ S. Saitoh,¹⁰ Y. Sakai,¹⁰ H. Sakamoto,¹⁸
 T. R. Sarangi,¹⁰ M. Satapathy,⁵⁴ N. Sato,²⁴ O. Schneider,²⁰ J. Schümann,²⁹ C. Schwanda,¹³
 A. J. Schwartz,⁶ T. Seki,⁵⁰ S. Semenov,¹⁴ K. Senyo,²⁴ Y. Settai,⁵ R. Seuster,⁹
 M. E. Sevior,²³ T. Shibata,³² H. Shibuya,⁴⁵ B. Shwartz,² V. Sidorov,² V. Siegle,³⁸
 J. B. Singh,³⁵ A. Somov,⁶ N. Soni,³⁵ R. Stamen,¹⁰ S. Stanić,^{53,*} M. Starić,¹⁵ A. Sugi,²⁴

A. Sugiyama,³⁹ K. Sumisawa,³⁴ T. Sumiyoshi,⁵⁰ S. Suzuki,³⁹ S. Y. Suzuki,¹⁰ O. Tajima,¹⁰
F. Takasaki,¹⁰ K. Tamai,¹⁰ N. Tamura,³² K. Tanabe,⁴⁸ M. Tanaka,¹⁰ G. N. Taylor,²³
Y. Teramoto,³³ X. C. Tian,³⁶ S. Tokuda,²⁴ S. N. Tovey,²³ K. Trabelsi,⁹ T. Tsuboyama,¹⁰
T. Tsukamoto,¹⁰ K. Uchida,⁹ S. Uehara,¹⁰ T. Uglov,¹⁴ K. Ueno,²⁹ Y. Unno,³ S. Uno,¹⁰
Y. Ushiroda,¹⁰ G. Varner,⁹ K. E. Varvell,⁴³ S. Villa,²⁰ C. C. Wang,²⁹ C. H. Wang,²⁸
J. G. Wang,⁵⁵ M.-Z. Wang,²⁹ M. Watanabe,³² Y. Watanabe,⁴⁹ L. Widhalm,¹³
Q. L. Xie,¹² B. D. Yabsley,⁵⁵ A. Yamaguchi,⁴⁷ H. Yamamoto,⁴⁷ S. Yamamoto,⁵⁰
T. Yamanaka,³⁴ Y. Yamashita,³¹ M. Yamauchi,¹⁰ Heyoung Yang,⁴¹ P. Yeh,²⁹ J. Ying,³⁶
K. Yoshida,²⁴ Y. Yuan,¹² Y. Yusa,⁴⁷ H. Yuta,¹ S. L. Zang,¹² C. C. Zhang,¹² J. Zhang,¹⁰
L. M. Zhang,⁴⁰ Z. P. Zhang,⁴⁰ V. Zhilich,² T. Ziegler,³⁷ D. Žontar,^{21,15} and D. Zürcher²⁰

(The Belle Collaboration)

¹*Aomori University, Aomori*

²*Budker Institute of Nuclear Physics, Novosibirsk*

³*Chiba University, Chiba*

⁴*Chonnam National University, Kwangju*

⁵*Chuo University, Tokyo*

⁶*University of Cincinnati, Cincinnati, Ohio 45221*

⁷*University of Frankfurt, Frankfurt*

⁸*Gyeongsang National University, Chinju*

⁹*University of Hawaii, Honolulu, Hawaii 96822*

¹⁰*High Energy Accelerator Research Organization (KEK), Tsukuba*

¹¹*Hiroshima Institute of Technology, Hiroshima*

¹²*Institute of High Energy Physics,*

Chinese Academy of Sciences, Beijing

¹³*Institute of High Energy Physics, Vienna*

¹⁴*Institute for Theoretical and Experimental Physics, Moscow*

¹⁵*J. Stefan Institute, Ljubljana*

¹⁶*Kanagawa University, Yokohama*

¹⁷*Korea University, Seoul*

¹⁸*Kyoto University, Kyoto*

¹⁹*Kyungpook National University, Taegu*

²⁰*Swiss Federal Institute of Technology of Lausanne, EPFL, Lausanne*

²¹*University of Ljubljana, Ljubljana*

²²*University of Maribor, Maribor*

²³*University of Melbourne, Victoria*

²⁴*Nagoya University, Nagoya*

²⁵*Nara Women's University, Nara*

²⁶*National Central University, Chung-li*

²⁷*National Kaohsiung Normal University, Kaohsiung*

²⁸*National United University, Miao Li*

²⁹*Department of Physics, National Taiwan University, Taipei*

³⁰*H. Niewodniczanski Institute of Nuclear Physics, Krakow*

³¹*Nihon Dental College, Niigata*

³²*Niigata University, Niigata*

³³*Osaka City University, Osaka*

³⁴*Osaka University, Osaka*

- ³⁵Panjab University, Chandigarh
³⁶Peking University, Beijing
³⁷Princeton University, Princeton, New Jersey 08545
³⁸RIKEN BNL Research Center, Upton, New York 11973
³⁹Saga University, Saga
⁴⁰University of Science and Technology of China, Hefei
⁴¹Seoul National University, Seoul
⁴²Sungkyunkwan University, Suwon
⁴³University of Sydney, Sydney NSW
⁴⁴Tata Institute of Fundamental Research, Bombay
⁴⁵Toho University, Funabashi
⁴⁶Tohoku Gakuin University, Tagajo
⁴⁷Tohoku University, Sendai
⁴⁸Department of Physics, University of Tokyo, Tokyo
⁴⁹Tokyo Institute of Technology, Tokyo
⁵⁰Tokyo Metropolitan University, Tokyo
⁵¹Tokyo University of Agriculture and Technology, Tokyo
⁵²Toyama National College of Maritime Technology, Toyama
⁵³University of Tsukuba, Tsukuba
⁵⁴Utkal University, Bhubaneswar
⁵⁵Virginia Polytechnic Institute and State University, Blacksburg, Virginia 24061
⁵⁶Yonsei University, Seoul

Abstract

We report a measurement of the first and second moment of the hadronic mass distribution M_X in $B \rightarrow X_{c\bar{c}}\nu$ decays for lepton threshold momenta ranging from 0.9 to 1.6 GeV/ c in the center of mass frame. The measurement uses $B\bar{B}$ events in which the hadronic decay of one B meson is fully reconstructed and a charged lepton from the decay of the other B meson is identified. These results are obtained from a 140 fb^{-1} data sample collected near the $\Upsilon(4S)$ resonance with the Belle detector at the KEKB asymmetric energy e^+e^- collider.

PACS numbers: 13.20.He,14.40.Nd

The heavy quark effective theory (HQET) combined with the operator product expansion provides a framework in which inclusive B decay properties can be calculated. In particular, the moments of various inclusive quantities in $B \rightarrow X_c \ell \nu$ decays, such as the lepton momentum p_ℓ , the 4-momentum transfer squared q^2 and the hadronic recoil mass M_X , can be related to the non-perturbative parameters that also appear in calculations of the semileptonic decay rate (see Ref. [1, 2, 3] for calculations of the moments of M_X). Measurements of these moments can thus improve calculations of the semileptonic B decay rate and lead to a more precise determination of the magnitude of the Cabibbo-Kobayashi-Maskawa (CKM) matrix element V_{cb} [4]. In this paper, we present a measurement of the first and second moment of M_X , $\langle M_X \rangle$ and $\langle M_X^2 \rangle$, for lepton momentum thresholds ranging from 0.9 to 1.6 GeV/ c in the center-of-mass (c.m.) frame.

The analysis is based on the data recorded with the Belle detector [5] at the asymmetric energy e^+e^- collider KEKB [6], operating at a c.m. energy near the $\Upsilon(4S)$ resonance. KEKB consists of a low energy ring (LER) of 3.5 GeV positrons and a high energy ring (HER) of 8 GeV electrons. The Belle detector is a large-solid-angle magnetic spectrometer consisting of a three-layer silicon vertex detector (SVD), a 50-layer central drift chamber (CDC), an array of aerogel threshold Čerenkov counters (ACC), a barrel-like arrangement of time-of-flight scintillation counters (TOF), and an electromagnetic calorimeter comprised of CsI(Tl) crystals (ECL) located inside a super-conducting solenoid coil that provides a 1.5 T magnetic field. The responses of the ECL, CDC (dE/dx) and ACC detectors are combined to provide clean electron identification. Muons are identified in the instrumented iron flux-return (KLM) located outside of the coil. Charged hadron identification relies on the information from the CDC, ACC and TOF sub-detectors.

The $\Upsilon(4S)$ dataset used for this study corresponds to an integrated luminosity of 140 fb $^{-1}$, or about 152 million $B\bar{B}$ events. Another 15 fb $^{-1}$ taken 60 MeV below the resonance are used to subtract the non- $B\bar{B}$ background. Full detector simulation based on GEANT [7] is applied to Monte Carlo (MC) simulated events. The size of the MC samples is equivalent to about three times the integrated luminosity. The decay $B \rightarrow D^* \ell \nu$ is simulated using a HQET-based model [8]. The ISGW2 model [9] is used for the decays $B \rightarrow D \ell \nu$ and $B \rightarrow D^{**} \ell \nu$. The non-resonant $B \rightarrow D^{(*)} \pi \ell \nu$ component is generated according to the model of Goity and Roberts [10].

We use $B\bar{B}$ events in which the hadronic decay of one B meson is fully reconstructed (B_{tag}) and the semileptonic decay of the recoiling B meson (B_{signal}) is inferred from the presence of a charged lepton (electron or muon). After selecting hadronic events [11], we reconstruct B_{tag} by searching the decay modes $B^+ \rightarrow \bar{D}^{(*)0} \pi^+, \bar{D}^{(*)0} \rho^+, \bar{D}^{(*)0} a_1^+$ and $B^0 \rightarrow D^{(*)-} \pi^+, D^{(*)-} \rho^+, D^{(*)-} a_1^+$ [12]. Pairs of photons satisfying $E_\gamma > 50$ MeV and $117 \text{ MeV}/c^2 < m(\gamma\gamma) < 150 \text{ MeV}/c^2$ are combined to form π^0 candidates. K_S^0 mesons are reconstructed from pairs of oppositely charged tracks with invariant mass within $\pm 30 \text{ MeV}/c^2$ of the K_S^0 mass and decay vertex displaced from the interaction point. Candidate ρ^+ and ρ^0 mesons are reconstructed in the $\pi^+\pi^0$ and $\pi^+\pi^-$ decay modes, requiring their invariant masses to be within $\pm 150 \text{ MeV}/c^2$ of the ρ mass. Candidate a_1^+ mesons are obtained by combining a ρ^0 candidate with a charged pion and requiring an invariant mass between 1.0 and 1.6 GeV/ c^2 . D^0 candidates are searched for in the $K^-\pi^+$, $K^-\pi^+\pi^0$, $K^-\pi^+\pi^+\pi^-$, $K_S^0\pi^+\pi^-$ and $K_S^0\pi^0$ decay modes. The $K^-\pi^+\pi^+$ and $K_S^0\pi^+$ modes are used to reconstruct D^+ mesons. Charmed mesons are selected in a window corresponding to ± 3 times the mass resolution in the respective decay mode. D^{*+} mesons are reconstructed by pairing a charmed meson with a low momentum pion, $D^{*+} \rightarrow D^0\pi^+, D^+\pi^0$. The decay modes $D^{*0} \rightarrow D^0\pi^0$

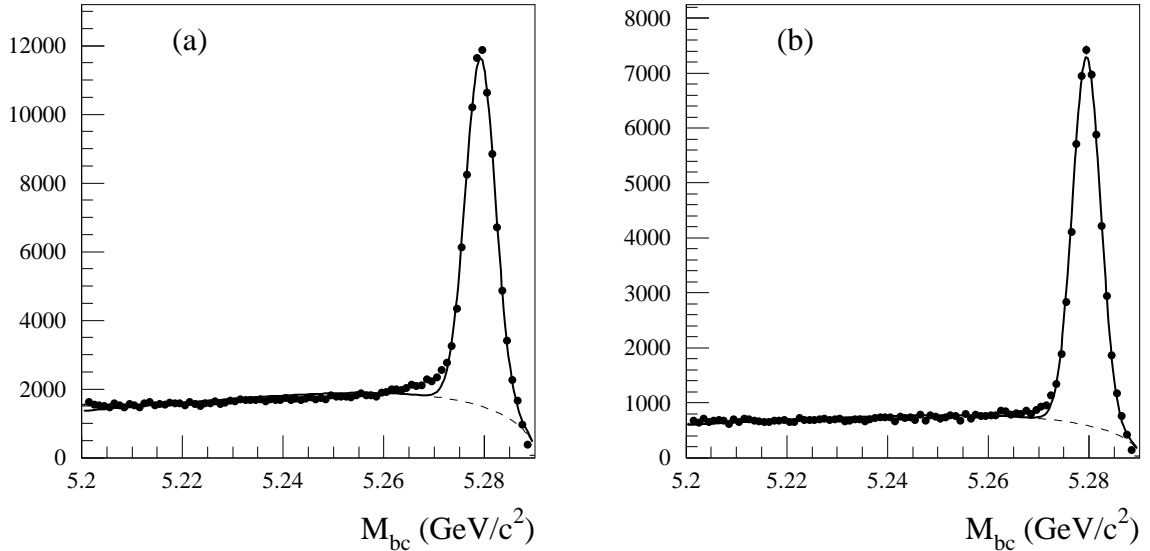


FIG. 1: Reconstruction of the tag-side B meson. The M_{bc} distribution after requiring $\Delta E < 50$ MeV is shown for fully reconstructed (a) B^+ (b) B^0 decays. The fit uses a Gaussian function for the signal component and an ARGUS background function [14] for the combinatorial background.

and $D^{*0} \rightarrow D^0\gamma$ are used to search for neutral charmed vector mesons.

For each B_{tag} candidate, the beam-constrained mass M_{bc} and ΔE are calculated [13]

$$M_{bc} = \sqrt{(E_{beam}^*)^2 - (\vec{p}_B^*)^2}, \quad \Delta E = E_B^* - E_{beam}^*, \quad (1)$$

where E_{beam}^* is the beam energy in the c.m. system, \vec{p}_B^* and E_B^* are the 3-momentum and the energy of the B_{tag} candidate, respectively. The signal region for B_{tag} is defined by the selections $M_{bc} > 5.27$ GeV/ c^2 and $\Delta E < 50$ MeV. If multiple candidates are found in a single event, the best candidate is chosen based on ΔE and other variables. Fig. 1 shows the M_{bc} distribution for $\Delta E < 50$ MeV. The number of the fully reconstructed B^+ (B^0) events, obtained by fitting this distribution with the sum of a Gaussian function for the signal component and an ARGUS background function [14], is $76, 155 \pm 511$ ($46, 863 \pm 374$) with a purity of the 74% (81%).

Semileptonic decays of B_{signal} are selected by requiring exactly one identified charged lepton among the particles that are not associated to B_{tag} . In the lepton momentum range relevant to this analysis, electrons (muons) are selected with an efficiency of 92% (89%) and the probability to misidentify a pion as an electron (a muon) is 0.25% (1.4%) [15, 16]. For B^+ tags, we require $Q_\ell \cdot Q_B < 0$, where Q_ℓ and Q_B are the charges of the lepton and of B_{tag} , respectively.

The charged tracks and neutral clusters which are associated neither with B_{tag} nor with the charged lepton are assigned to the hadronic X system. The 4-momenta of the charged particles are calculated with the pion mass except for identified kaons. The missing 4-momentum in the event is calculated,

$$\mathbf{p}_{\text{miss}} = (p_{\text{LER}} + p_{\text{HER}}) - p_{B_{tag}} - p_\ell - p_X, \quad (2)$$

where the indices LER and HER refer to the colliding beams. As only the neutrino in

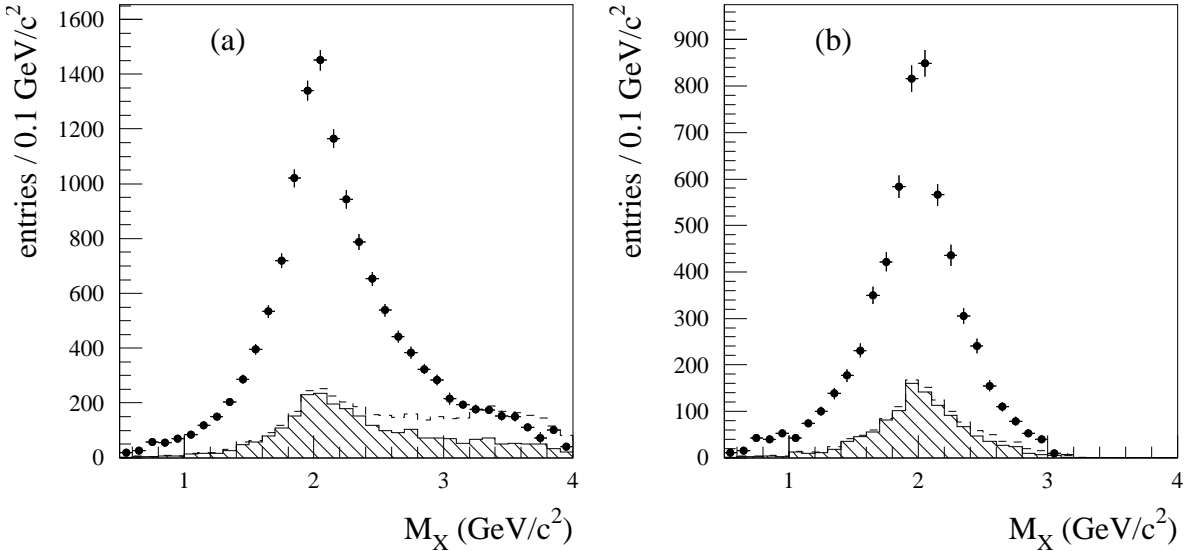


FIG. 2: The M_X distributions for (a) $p_\ell^* > 0.9 \text{ GeV}/c$ and (b) $p_\ell^* > 1.6 \text{ GeV}/c$. The data points are the $\Upsilon(4S)$ data after subtraction of the non- $B\bar{B}$ background. The background from secondary or misidentified leptons is indicated by the dashed line. The combinatorial background in the B_{tag} sample is shown as a hatched histogram.

$B \rightarrow X_c \ell \nu$ should be missing in the event, we require the missing mass to be consistent with zero, $|M_{\text{miss}}^2| < 2 \text{ GeV}^2/c^4$.

The neutrino 4-momentum is inferred from the missing momentum, $p_\nu = (|\vec{p}_{\text{miss}}|, \vec{p}_{\text{miss}})$, and the 4-momentum of the X system is recalculated,

$$p'_X = (p_{\text{LER}} + p_{\text{HER}}) - p_{B_{\text{tag}}} - p_\ell - p_\nu . \quad (3)$$

The M_X resolution (defined as half width at the half maximum) obtained with this procedure is about $200 \text{ MeV}/c^2$.

The background consists of the following components: combinatorial background in the B_{tag} sample, background from secondary or misidentified leptons, and background from non- $B\bar{B}$ events. The combinatorial background is dominant. Its shape (in M_X and M_X^2) is determined from the MC simulation, and the M_{bc} side-band region ($5.2 \text{ GeV}/c^2 < M_{bc} < 5.27 \text{ GeV}/c^2$, $|\Delta E| < 50 \text{ MeV}$) is used to determine its normalization, separately for each lepton momentum threshold. The background from secondary or misidentified leptons is significant in the low lepton momentum region. Its shape is estimated from the MC simulation, and the number of well-reconstructed B_{tag} candidates is used for its normalization. The magnitude of the background from misidentified leptons is corrected using the pion misidentification rate measured in $K_S^0 \rightarrow \pi^+ \pi^-$ decays in hadronic events. The background from non- $B\bar{B}$ events is smallest, and it is subtracted using the data taken 60 MeV below the $\Upsilon(4S)$ resonance. Fig. 2 shows the M_X distributions for different minimum lepton momenta in the c.m. frame, together with the background estimation.

To correct for the distortions caused by finite detector resolution, the background-subtracted M_X and M_X^2 distributions are unfolded using the Singular Value Decomposition (SVD) algorithm [17]. The approach consists in describing the detector response by a correlation matrix between the true and the reconstructed M_X (M_X^2) values which is determined

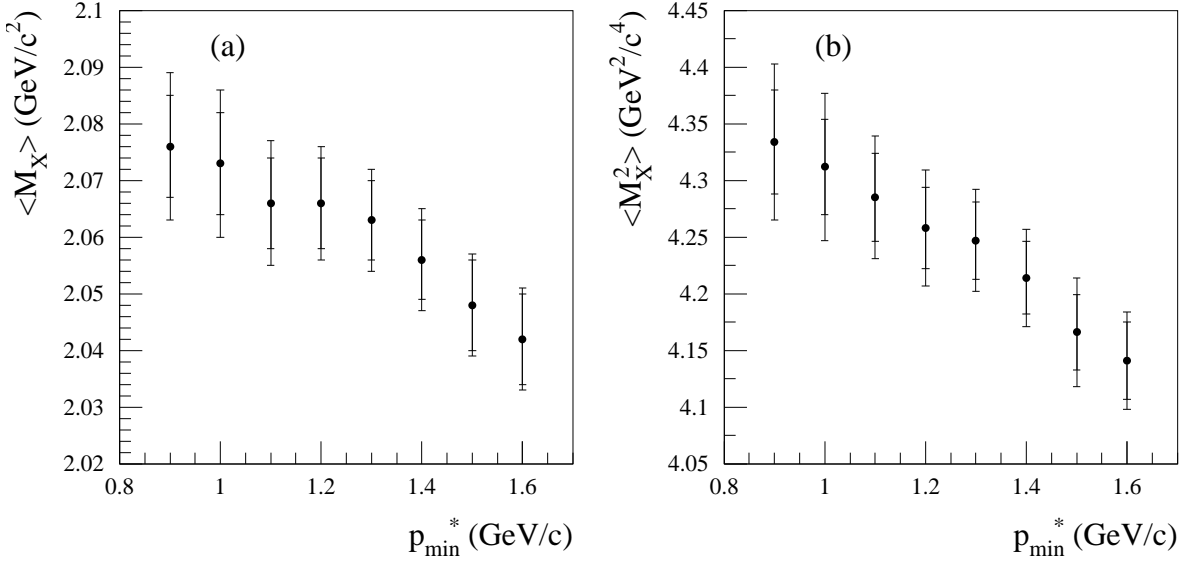


FIG. 3: The first and second hadronic mass moments, $\langle M_X \rangle$ and $\langle M_X^2 \rangle$, for different lepton threshold momenta. The error bars indicate the statistical and total errors. Note that the individual moments are highly correlated. All results are preliminary.

from the MC simulation. This matrix is decomposed into its eigenvalue components, and only the contributions leading to a statistically stable solution are kept. For the unfolding of the M_X (M_X^2) distribution, the measured spectrum is divided into 35 (39) 0.1 GeV/c^2 (0.333 GeV^2/c^4) wide bins. For the unfolded distribution, 12 (13) bins are used.

For each minimum lepton momentum, ranging from 0.9 to 1.6 GeV/c , the background-subtracted M_X and M_X^2 distributions are unfolded, separately for B^+ and B^0 tags, and for electron and muon events. For each of these four sub-samples, the values of $\langle M_X \rangle$ and $\langle M_X^2 \rangle$ are obtained by calculating the mean values of the unfolded M_X and M_X^2 distributions. The results obtained by averaging the four sub-sample results are shown in Fig. 3 and Tables I and II. All results are preliminary. This procedure has been tested on MC simulated events for the full minimum lepton momentum range and no significant bias has been found.

We consider three sources of systematic error, shown separately in columns three to five of Tables I and II: uncertainty related to detector modeling and residual background subtraction, uncertainty related to the unfolding procedure, and uncertainty related to the X_c model in the MC simulation. The total systematic error quoted on the moments corresponds to the quadratic sum of these three components.

The uncertainty related to the detector modeling and to the background subtraction is estimated from the consistency between the four sub-samples, by varying the selections used in the analysis (namely the B_{tag} signal region and the requirement on M_{miss}^2), and by varying the background normalization. The uncertainty related to the unfolding procedure is estimated by changing the number of eigenvalue components in the unfolding solution. The X_c model uncertainty is obtained by varying the fractions of $B \rightarrow D^* \ell \nu$, $B \rightarrow D \ell \nu$ and $B \rightarrow D^{**}/D^{(*)} \pi \ell \nu$ within $\pm 10\%$, $\pm 10\%$ and $\pm 30\%$, respectively, and summing the individual variations in quadrature. These ranges of variation roughly correspond to the experimental uncertainties [18] in the isospin averaged branching ratios.

In summary, we have performed a measurement of the first and second moment of the

p_{min}^* (GeV/c)	$\langle M_X \rangle$ (GeV/ c^2)	Detector/ background	Unfolding	X_c model
0.9	$2.076 \pm 0.009 \pm 0.010$	0.006	0.008	0.003
1.0	$2.073 \pm 0.009 \pm 0.010$	0.005	0.008	0.003
1.1	$2.066 \pm 0.008 \pm 0.008$	0.005	0.005	0.003
1.2	$2.066 \pm 0.008 \pm 0.006$	0.004	0.004	0.003
1.3	$2.063 \pm 0.007 \pm 0.006$	0.004	0.005	0.003
1.4	$2.056 \pm 0.007 \pm 0.006$	0.003	0.004	0.003
1.5	$2.048 \pm 0.008 \pm 0.005$	0.003	0.003	0.002
1.6	$2.042 \pm 0.008 \pm 0.004$	0.003	0.001	0.002

TABLE I: The first hadronic mass moment $\langle M_X \rangle$ for different lepton threshold momenta. The first error on $\langle M_X \rangle$ is statistical and the second is total systematic uncertainty, *i.e.*, the quadratic sum of the right-most three columns. All results are preliminary.

p_{min}^* (GeV/c)	$\langle M_X^2 \rangle$ (GeV $^2/c^4$)	Detector/ background	Unfolding	X_c model
0.9	$4.334 \pm 0.046 \pm 0.051$	0.041	0.027	0.014
1.0	$4.312 \pm 0.042 \pm 0.049$	0.037	0.030	0.013
1.1	$4.285 \pm 0.039 \pm 0.037$	0.032	0.017	0.012
1.2	$4.258 \pm 0.036 \pm 0.036$	0.027	0.021	0.012
1.3	$4.247 \pm 0.034 \pm 0.030$	0.023	0.016	0.011
1.4	$4.214 \pm 0.032 \pm 0.028$	0.024	0.009	0.011
1.5	$4.166 \pm 0.033 \pm 0.035$	0.022	0.025	0.011
1.6	$4.141 \pm 0.034 \pm 0.027$	0.022	0.010	0.013

TABLE II: The second hadronic mass moment $\langle M_X^2 \rangle$ for different lepton threshold momenta. The first error on $\langle M_X^2 \rangle$ is statistical and the second is total systematic uncertainty, *i.e.*, the quadratic sum of the right-most three columns. All results are preliminary.

hadronic mass distribution M_X in $B \rightarrow X_c \ell \nu$ decays for minimum lepton momenta ranging from 0.9 to 1.6 GeV/c in the c.m. frame. The results listed in Tables I and II are compatible with recent values from other experiments [20, 21]. It is expected that this measurement (combined with measurements of the semileptonic branching fraction and of the moments of the lepton spectrum in $B \rightarrow X_c \ell \nu$) will lead to an improved determination of the CKM matrix element $|V_{cb}|$.

We thank the KEKB group for the excellent operation of the accelerator, the KEK Cryogenics group for the efficient operation of the solenoid, and the KEK computer group and the National Institute of Informatics for valuable computing and Super-SINET network support. We acknowledge support from the Ministry of Education, Culture, Sports, Science, and Technology of Japan and the Japan Society for the Promotion of Science; the Australian

Research Council and the Australian Department of Education, Science and Training; the National Science Foundation of China under contract No. 10175071; the Department of Science and Technology of India; the BK21 program of the Ministry of Education of Korea and the CHEP SRC program of the Korea Science and Engineering Foundation; the Polish State Committee for Scientific Research under contract No. 2P03B 01324; the Ministry of Science and Technology of the Russian Federation; the Ministry of Education, Science and Sport of the Republic of Slovenia; the National Science Council and the Ministry of Education of Taiwan; and the U.S. Department of Energy.

* on leave from Nova Gorica Polytechnic, Nova Gorica

- [1] P. Gambino and N. Uraltsev, Eur. Phys. J. **C 34**, 181 (2004).
- [2] A. Falk and M. Luke, Phys. Rev. **D 57**, 424 (1998).
- [3] A. Falk, M. Luke and M. Savage, Phys. Rev. **D 53**, 2491 (1996); *ibid.* **53**, 6316 (1996).
- [4] M. Kobayashi and T. Maskawa, Prog. Theor. Phys. **49**, 652 (1973).
- [5] A. Abashian *et al.* (Belle Collaboration), Nucl. Instr. and Meth. **A 479**, 117 (2002).
- [6] S. Kurokawa and E. Kikutani, Nucl. Instr. and Meth. **A 499**, 1 (2003), and other papers included in this volume.
- [7] R. Brun *et al.*, GEANT 3.21, CERN Report DD/EE/84-1 (1984).
- [8] J. Duboscq *et al.* (CLEO Collaboration), Phys. Rev. Lett. **76**, 3898 (1996).
- [9] N. Isgur and D. Scora, Phys. Rev. **D 52**, 2783 (1995). See also N. Isgur *et al.*, Phys. Rev. **D 39**, 799 (1989).
- [10] J.L. Goity and W. Roberts, Phys. Rev. **D 51**, 3459 (1995).
- [11] The selection of hadronic events is described in K. Abe *et al.* (Belle Collaboration), Phys. Rev. **D 64**, 072001 (2001).
- [12] Throughout this paper, the inclusion of the charge conjugate mode is implied.
- [13] Throughout this paper, quantities calculated in the c.m. frame are denoted by an asterisk.
- [14] H. Albrecht *et al.* (ARGUS Collaboration), Phys. Lett. **B 241**, 278 (1990).
- [15] K. Hanagaki *et al.*, Nucl. Instr. and Meth. **A 485**, 490 (2002).
- [16] A. Abashian *et al.*, Nucl. Instr. and Meth. **A 491**, 69 (2002).
- [17] A. Höcker and V. Kartvelishvili, Nucl. Instr. Meth. **A372**, 469 (1996).
- [18] S. Eidelman *et al.*, Phys. Lett. **B592**, 1 (2004).
- [19] M. Battaglia *et al.* (DELPHI Collaboration), DELPHI 2003-028 CONF 648.
- [20] S.E. Csorna *et al.* (CLEO Collaboration), Phys. Rev. **D 70**, 032002 (2004).
- [21] B. Aubert *et al.* (BABAR Collaboration), Phys. Rev. **D 69**, 111103 (2004).